Bridge Maintenance, Safety, Management, Digitalization and Sustainability – Jensen, Frangopol & Schmidt (eds)

Dynamic substructuring technique for submerged floating tunnels

S. Corazza, F. Foti & L. Martinelli
Department of Civil and Environmental Engineering, Politecnico di Milano, Italy

ABSTRACT: Seabed-anchored Submerged Floating Tunnels (SFTs) are structures made of watertight tubular segments, assembled, and kept floating under the water table by a spread system of anchoring elements connected to the seabed. Due to their inherent flexibility, SFTs are prone to the effect of dynamic loads such as seismic and hydrodynamic loads. These peculiar features have since long lead to the assessment of the SFTs' dynamic response by resorting to the simplified model of a beam on an elastic foundation. This amounts to totally neglect the mass of the anchoring elements and, therefore, their local vibration modes. In this work, the mooring system is modeled as a discrete series of taut-strings possessing axial extensibility, while the tunnel is considered as a continuous Euler-Bernoulli beam. Within this modeling choices, a dynamic substructuring technique is presented and used to obtain both the natural circular frequencies and the mode shapes of the coupled system.

1 INTRODUCTION

Submerged Floating Tunnels (SFTs) are an interesting alternative to long-span bridges and immersed tunnels for crossing deep waterways. Their origin can be traced back to the first patents granted in Norway in 1923-1947 (see (Jacobsen 2010)). Even though a first realization is still missing, preliminary design proposals have been developed for sea straits, fjords and lakes (see, e.g. (Ahrens 1997), (Bruschi et al. 1990)). A distinctive feature of the dynamic behavior of SFTs is the presence of both global vibration modes, that involve significant displacements of the tunnel and quasi-static displacements of the anchoring elements, and local modes, that mainly involve transverse vibrations of the anchors. Dominant global and local modes of the structure are typically associated to well-separated values of the natural frequencies. However, computationally efficient Finite Element (FE) models able to simultaneously capture the main features of both global and local vibration modes with the same degree of accuracy, are inherently hard to set up. To overcome this difficulty, a dynamic substructuring technique for SFTs is here presented. A separate modeling of the two main substructures (i.e. the tunnel and the mooring system) is employed, involving (1) a Reduced Order Model (ROM) of the anchoring elements, which accounts for a generic form of support motion, and (2) a continuous model of the tunnel, which relies on the well-known Euler-Bernoulli beam theory. Within this context, undamped free vibrations of the coupled system are studied, evidencing the influence of a variable mooring stiffness profile on the mode shapes of the SFT, and shedding light on the effect of the mooring system's mass on the global response of the structure. As an illustrative example, the aforementioned approach is applied to the SFT proposal for the Messina's strait crossing, in Italy. On this behalf, the classification of the SFT motion regimes is investigated with regards to the spectral description of hydrodynamic loads, that are assumed to be representative of both service life conditions of the structure and extreme events. The paper is organized as follows: the modeling of the two substructures is presented in Section 2, then the global equations of motion of the SFT are derived in Section 3.

DOI: 10.1201/9781003483755-119

An application example regarding the proposal for the Messina's strait SFT is presented in Section 4, while the conclusions of the work are drawn in Section 5.

2 SUBSTRUCTURES MODELING

2.1 *Preliminaries*

Let us refer to Figure 1a, and consider a tether inclined with an angle θ with respect to the horizontal plane, having initial chord length L_0, external diameter D_o, mass per unit of length γ_s, axial stiffness EA_0 and subject to a static tension $T_0 > 0$ (i.e. a pretension). It is also convenient for the following developments to introduce the non-dimensional load parameter as $\eta_0 = T_0/T_y$, where $T_y = f_y A_0$ is the yielding tensile force and f_y is the yielding stress of the material. The non-dimensional load parameter is directly proportional to the Buoyancy-to-Weight Ratio (BWR) of the tunnel. Moreover, in the case of the vibrations of submerged anchoring elements, the structural linear mass should be modified to account for the mass of the fluid which is moved due to the presence of the anchoring element itself (i.e. the so-called added mass), resulting in "virtual" mass per unit of length given by:

$$\gamma_v = \gamma_s + C_A \gamma_w \tag{1}$$

where γ_w denotes the linear mass of the water moved by a "section" of the tether (i.e. $\gamma_w = \rho_w \pi D_o^2/4$) and C_A denotes the added-mass coefficient, which depends on the cable cross-section. In the case of a circular cross-section, the unit value is usually adopted (i.e. C_A =1) (see, e.g. (Chakrabarti 1987)).

2.2 *Reduced-order model of the anchoring elements*

the anchoring elements of the mooring system are described according to a slightly modified version of the classical taut-string model. Indeed, sag effects and geometrical nonlinearities are neglected, while axial extensibility is accounted for in the present work. It is worth noticing that the well-known elasto-geometric Irvine's parameter (often denoted as λ^2), which is introduced when dealing with the small-sag cable theory, is strictly equal to zero for the present modeling choice, being the initial static configuration coincident with the reference (undeformed) configuration, i.e. the chord of the tether. Let us denote with u_a and w_a the interface-degrees of freedom associated to the top support motion of the anchoring element, according to a classical dynamic substructuring framework, and collect them in a vector $\boldsymbol{r}^k = [u^k{}_a,\ w^k{}_a]^{\mathrm{T}}$, where the superscript k denotes the generic k-th anchoring element. The work-conjugated quantities to the support displacements are the interface forces Fu_a and Fw_a, which can be casted in the following vector: $\boldsymbol{R}^k = [Fu_a{}^k,\ Fw_a{}^k]^{\mathrm{T}}$. In this work, the bottom support is kept fixed to the seabed; however, generalization of the proposed approach to account for soil-structure interaction phenomena is straightforward.

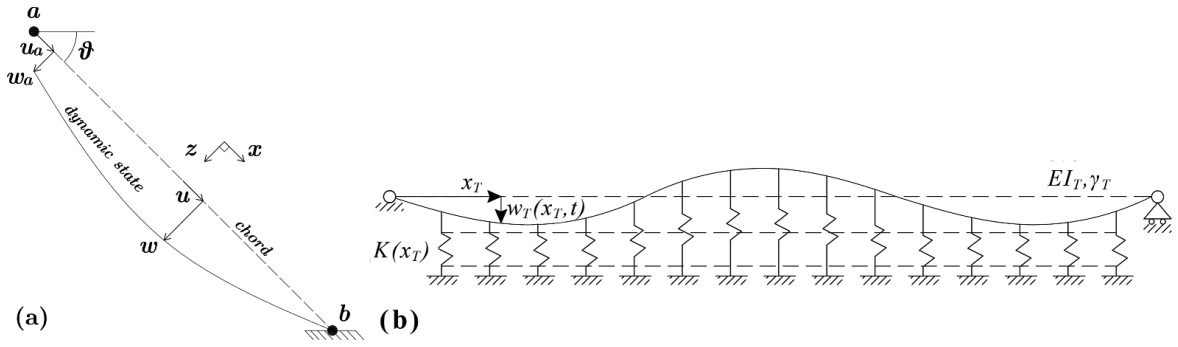

Figure 1. Schematic representation of a generic anchoring element (a), schematic representation of the SFT modeled as an Euler-Bernoulli beam on a Winkler's bed (b).

By following the approach proposed by (Warnitchai et al. 1995), the total motion of the anchoring element is decomposed in a quasi-static component (superscript q) and a modal component (superscript m). The longitudinal and transverse displacement respectively reads:

$$u(x,t) = u^q(x,t) + u^m(x,t) \tag{2}$$

$$w(x,t) = w^q(x,t) + w^m(x,t) \tag{3}$$

At this stage, the quasi-static component of the motion can be related to the support displacements by means of suitable shape functions, whereas the modal part can be expressed as a function of time-varying modal coordinates. Moreover, the axial modal motion can be neglected, being the frequencies of such motion much higher than the ones associated to the flexural motion, i.e.: $u^m(x,t) \ll w^m(x,t)$. One then has:

$$w(x,t) = \sum_{s=1}^{N_r} \psi_{w,s}(x) r_s(t) + \sum_{m=1}^{M} \phi_m(x) z_m(t) \tag{4}$$

$$u(x,t) = \sum_{s=1}^{N_r} \psi_{u,s}(x) r_s(t) \tag{5}$$

The shape functions of the quasi-static component of the motion (i.e. $\psi_{w,s}$ and $\psi_{u,s}$) are linear functions of the interface degrees of freedom r_s, i.e. the entries of the vector $\boldsymbol{r}^k$ (being N_r the total number of interface degrees of freedom. In this case $N_r = 2$), while the modal shape functions are selected as the fixed-base eigenmodes of the taut-string (see e.g. (Irvine 1981)):

$$\phi_m(x) = \sin\frac{m\pi x}{L_0} \tag{6}$$

According to a classical lagrangian approach, the kinetic and potential energy of the generic anchoring element can be respectively expressed as:

$$\mathrm{K}(t) = \frac{1}{2}\gamma_v \int_0^{L_0} \left[\left(\frac{\partial u}{\partial t}\right)^2 + \left(\frac{\partial w}{\partial t}\right)^2 \right] dx \tag{7}$$

$$V(t) = \frac{1}{2} EA_0 \int_0^{L_0} \varepsilon^2(x) dx + \frac{1}{2} T_0 \int_0^{L_0} \left[\left(\frac{\partial u}{\partial x}\right)^2 + \left(\frac{\partial w}{\partial x}\right)^2 \right] dx \tag{8}$$

where, by denoting with an apex the total derivative operator, the axial strain reads:

$$\varepsilon(x) = \frac{\partial u(x,t)}{\partial x} = \sum_{s=1}^{N_r} \psi'_{u,s}(x) r_s(t) \tag{9}$$

Substitution of Equations (4), (5) and (9) into Equations (7) and (8) straightforwardly leads to the identification of the entries of both mass and stiffness matrices. The undamped equation of motion (in partitioned form) of the k-th anchoring element simply reads:

$$\begin{bmatrix} \boldsymbol{M}^k_{rr} & \boldsymbol{M}^k_{rz} \\ \boldsymbol{M}^k_{zr} & \boldsymbol{M}^k_{zz} \end{bmatrix} \begin{bmatrix} \ddot{\boldsymbol{r}}^k \\ \ddot{\boldsymbol{z}}^k \end{bmatrix} + \begin{bmatrix} \boldsymbol{K}^k_{rr} & \boldsymbol{K}^k_{rz} \\ \boldsymbol{K}^k_{zr} & \boldsymbol{K}^k_{zz} \end{bmatrix} \begin{bmatrix} \boldsymbol{r}^k \\ \boldsymbol{z}^k \end{bmatrix} = \begin{bmatrix} \boldsymbol{R}^k \\ \boldsymbol{F}^k_z \end{bmatrix} \tag{10}$$

where $\boldsymbol{z}^k$ is vector containing the modal coordinates of the k-th anchoring element, i.e.: $\boldsymbol{z}^k = [z_1,\ldots,z_m,\ldots,z_M]^{\mathrm{T}}$ and $\boldsymbol{F}^k_z = [F_1,\ldots,F_m,\ldots,F_M]^{\mathrm{T}}$ is the vector of modal generalized loads, whose components can be obtained through a direct projection on the modal basis of the external forces (e.g. hydrodynamic loads) acting on the k-th element.

2.3 *Tunnel modeling strategy*

The tunnel is modeled as a Euler-Bernoulli beam. Let us denote with L_T and D_T, respectively, the total length of the tunnel and its external diameter, with EI_T its flexural stiffness, and with γ_T its mass per unit of length, which is comprehensive of the added mass of the water moved by the tunnel itself (i.e. $\gamma_T = \gamma_{sT} + \rho_w \pi D_T^2/4$). Then, the vertical (i.e. in-plane, w_T) and horizontal (i.e. out-of-plane, v_T) displacements can be expanded in the modal basis of the decoupled tunnel (free-interface modes):

$$w_T(x_T, t) = \sum_{n=1}^{N_{in}} \phi_n(x_T) q_n(t) \tag{11}$$

$$v_T(x_T, t) = \sum_{n=1}^{N_{out}} \phi_n(x_T) p_n(t) \tag{12}$$

where q_n and p_n denote, respectively, the in-plane and out-of-plane generalized displacements, N_{in} and N_{out} denote, respectively, the in-plane and out-of-plane number of retained basis functions, and:

$$\phi_n = \sin \frac{n\pi x_T}{L_T} \tag{13}$$

being $x_T \in [0, L_T]$ an abscissa spanning the longitudinal dimension of the tunnel (see Figure 1(b)). Entries of both mass and stiffness matrices of the bare tunnel can be easily computed by resorting to classical expressions (see e.g. (Foti et al. 2023)). The undamped equation of motion of the tunnel reads:

$$\boldsymbol{M}_T \ddot{\boldsymbol{q}}_T + \boldsymbol{K}_T \boldsymbol{q}_T = \boldsymbol{F}_T - \sum_{k=1}^{N_A} \boldsymbol{\Phi}_A^k \boldsymbol{F}_k \tag{14}$$

where $\boldsymbol{q}_T = [\boldsymbol{p}, \boldsymbol{q}]^{\mathrm{T}}$ is the vector which collects the out-of-plane and in-plane generalized displacements of the tunnel, $\boldsymbol{F}_T$ is the vector of modal generalized dynamic loads which is obtained by direct projection of the external forces (e.g. hydrodynamic loads), on the modal basis of the tunnel, N_A is the total number of anchoring elements, $\boldsymbol{F}_k = [H_k, V_k]^{\mathrm{T}}$ is the vector containing the horizontal (H_k) and vertical (V_k) forces acting on the tunnel (exchanged by the k-th anchoring element) and $\boldsymbol{\Phi}_A^k$ is the matrix whose entries are defined as follows:

$$\boldsymbol{\Phi}_A^k = \begin{bmatrix} \sin\frac{\pi x_{A,k}}{L_T} & \dots & \sin\frac{n\pi x_{A,k}}{L_T} & \dots & \sin\frac{N_{out}\pi x_{A,k}}{L_T} & 0 & \dots & 0 & \dots & 0 \\ 0 & \dots & 0 & \dots & 0 & \sin\frac{\pi x_{A,k}}{L_T} & \dots & \sin\frac{n\pi x_{A,k}}{L_T} & \dots & \sin\frac{N_{in}\pi x_{A,k}}{L_T} \end{bmatrix} \tag{15}$$

being $x_{A,k}$ the abscissa of the k-th anchoring element in the reference system of the tunnel.

3 EQUATIONS OF MOTION OF THE SFT

In order to couple the equations of motion of the anchoring elements (see section 2.2) and those of the tunnel (see section 2.3), some further advancements are necessary. The interface forces exchanged between the anchoring elements and the tunnel can be expressed in a vectorial form as:

$$\boldsymbol{F}^k = \boldsymbol{T}_k \boldsymbol{R}^k \tag{16}$$

where $\boldsymbol{T}_k$ is the transformation matrix, which permits to pass from the local reference frame of the k-th anchoring element, to the global reference frame of the tunnel, which simply reads:

$$\boldsymbol{T_k} = \begin{bmatrix} \cos\theta_k & -\sin\theta_k \\ \sin\theta_k & \cos\theta_k \end{bmatrix} \tag{17}$$

It is noteworthy that in many SFT design proposals, the angle of inclination $\theta_k = \theta$ is constant for each anchoring element, resulting in a constant transformation matrix $\boldsymbol{T_k} = \boldsymbol{T}$ as well.

By resorting to the description of the displacement field of the tunnel, one can express the vector of interface displacements of the k-th anchoring element according to the following relationship:

$$\boldsymbol{r^k} = \boldsymbol{T}^T \boldsymbol{\Phi}_A^k \boldsymbol{q}_T \tag{18}$$

At this stage, Equation (18) is substituted into the system of Equations (10), and the vector of interface forces acting on the k-th anchor $\boldsymbol{R^k}$ is expressed from the first row. Direct substitution of $\boldsymbol{R^k}$ into Equation (16) allows to obtain the vector of interface forces acting on the tunnel, i.e. $\boldsymbol{F^k}$, which can be finally inserted into Equation (14). The undamped equations of motion of the SFT are then obtained by direct assembling the contributions stemming from all the (N_A) anchoring elements. The system of equations finally reads:

$$\begin{bmatrix} \boldsymbol{M}_T + \boldsymbol{\Phi}_A^T \boldsymbol{T} \boldsymbol{M}_{rr} \boldsymbol{T}^T \boldsymbol{\Phi}_A & \boldsymbol{\Phi}_A^T \boldsymbol{T} \boldsymbol{M}_{rz} \\ \boldsymbol{M}_{zr} \boldsymbol{T}^T \boldsymbol{\Phi}_A & \boldsymbol{M}_{zz} \end{bmatrix} \begin{bmatrix} \ddot{\boldsymbol{q}}_T \\ \ddot{\boldsymbol{z}} \end{bmatrix} + \begin{bmatrix} \boldsymbol{K}_T + \boldsymbol{\Phi}_A^T \boldsymbol{T} \boldsymbol{K}_{rr} \boldsymbol{T}^T \boldsymbol{\Phi}_A & 0 \\ 0 & \boldsymbol{K}_{zz} \end{bmatrix} \begin{bmatrix} \boldsymbol{q}_T \\ \boldsymbol{z} \end{bmatrix} = \begin{bmatrix} \boldsymbol{F}_T \\ \boldsymbol{F}_z \end{bmatrix} \tag{19}$$

where the matrices $\boldsymbol{\Phi}_A$, $\boldsymbol{T}$, $\boldsymbol{M}_{rr}$, $\boldsymbol{K}_{rr}$, $\boldsymbol{M}_{zz}$, $\boldsymbol{K}_{zz}$ and $\boldsymbol{M}_{rz}$ and the vectors $\boldsymbol{F}_T$ and $\boldsymbol{F}_z$ have been assembled by blocks, according to standard procedures (see e.g. (Clough and Penzien 2003)) and $\boldsymbol{z}$ is the vector obtained by queueing the vectors of modal coordinates $\boldsymbol{z_k}$ of each anchoring element. Circular frequencies and mode shapes of the SFT are then found from the following undamped eigenproblem:

$$\left(\boldsymbol{K}_G - \omega^2 \boldsymbol{M}_G\right)\varphi = 0 \tag{20}$$

where the global mass ($\boldsymbol{M_G}$) and stiffness ($\boldsymbol{K_G}$) matrices have been implicitly defined in Equation (19).

4 APPLICATION EXAMPLE

The present section considers an application example regarding the SFT which was proposed for the crossing of the Messina's strait, in Italy (see e.g. (Bruschi et al. 1990), (Perotti et al. 2018)). The considered SFT is designed to connect Sicily to the mainland, crossing a strait characterized by a maximum seabed depth of 325 m (see Figure 2). The total length of the SFT is L_T = 4680 m and the tunnel axis is placed 40 m below the water table. The cross section of the tunnel is defined by the following parameters: D_T = 15.95 m, $EI = 4.383 \cdot 10^{10}$ kNm^2 and γ_T = 368.41 ton/m. The mooring system is made of inclined hollow core circular cross-section tethers, located along 65 mooring stations, with uniform spacing equal to 72 m. For the sake of simplicity, in the present work, the mooring system is considered composed of one hollow circular cross-section only (Type B), leading to a mooring stiffness variability which is only induced by the variation of the seabed depth along the tunnel's abscissa. The cross-section type B is defined by the following parameters: D_o = 1.950 m, s = 0.065 m, A_0 = 0.3849 m^2, γ_v = 6005 kg/m, where s denotes the thickness of the hollow circular profile. The angle of inclination and the non-dimensional loading parameter of the anchoring elements are set respectively to θ= 45° and η_0 = 5%.

In the present work, only in-plane motion of the tunnel is considered, and 100 terms are retained in the series expansion of Equation (11) (i.e. N_{in} =100 and N_{out} = 0). The mooring system is modeled by considering 65 "equivalent" anchoring elements, i.e. characterized by values of both axial stiffness and virtual mass which are representative of the real configuration

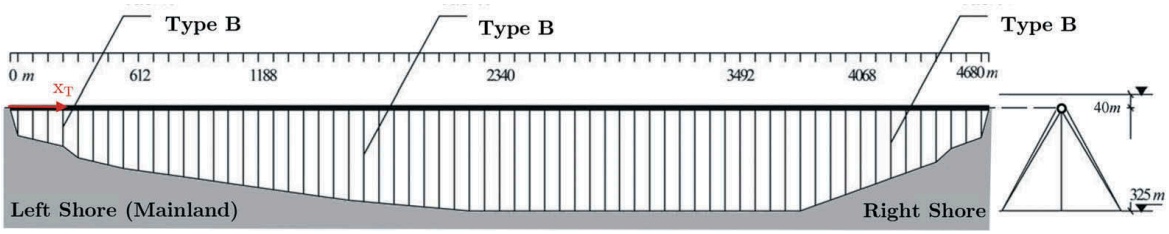

Figure 2. Side view and cross-section of the proposal for the Messina's strait SFT, in Italy.

(which is composed of 4 inclined tethers per mooring section, see again Figure 2). Each "equivalent" tether is then modeled by retaining the first in-plane mode only (i.e. M=1).

Hydrodynamic loads acting on the structure have been modeled starting from the spectral representation of the wave elevation for a certain return period. A general analytical form of the surface wave energy spectrum is (see e.g. (Wilson 1984)):

$$S_\eta(\omega) = C_0 \omega^{-m} e^{-B\omega^{-n}} \tag{21}$$

in which the empirical coefficients C_0, B, m and n define the spectrum. In the most widely used forms, m = 5 and n = 4. Several empirical expressions for the C_0 and B coefficients have been proposed in the literature. In the following, reference is made to the so-called Bretschneider Spectrum, for which C_0 and B coefficients become:

$$C_0 = 0.0081 g^2$$
$$B = 3.11/H_s^2 \tag{22}$$

where g is the gravity acceleration and H_s is the significant wave height. The latter is an important statistical parameter defined as the arithmetic average of the highest one-third of the waves in a wave record (Wilson 1984). Two significant wave heights are considered for the following developments, namely H_s = 5 m and H_s = 16 m, which are tentatively assumed to represent the "operational" wave conditions and extreme hydrodynamic events, respectively.

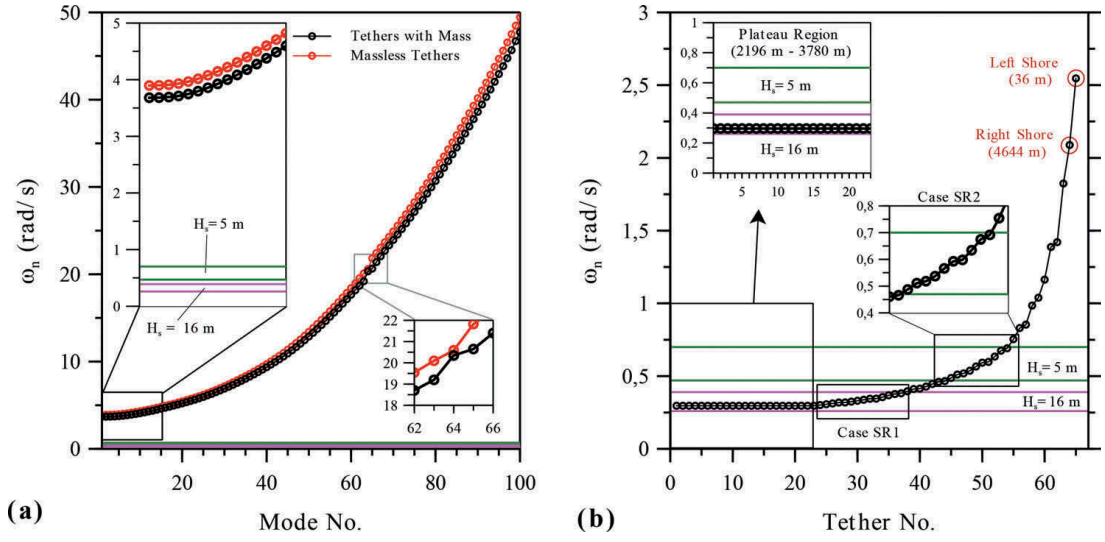

Figure 3. Natural circular frequencies of the tunnel (a) and of the anchoring elements (b) compared to the band of circular frequencies associated to the highest wave elevation spectral ordinates, for two significant wave heights (H_s = 5 m and H_s = 16 m).

Figure 3a depicts the tunnel circular frequencies obtained from the solution of the eigenvalue problem (see Equation (21)) compared to the ones corresponding to the highest spectral ordinates

of the wave elevation spectrum S_η. As a first important comment, it is evident that the response of the tunnel to hydrodynamic excitation can be regarded as quasi-static, being the first natural frequency of the tunnel much higher than the frequency interval associated to the highest spectral ordinates of the wave spectra. Additionally, it is noted that accounting for the anchoring elements' mass, leads to a variation of about 5.5% in the tunnel's circular frequencies, compared to the massless tethers modeling choice. Moreover, around mode 65, an abrupt change in the frequency can be observed. This phenomenon is due to the matching of the wavelength of such mode and the spacing of the anchoring elements, resulting in an activation of the quasi-static motion of the whole mooring system, with a consequent increased global stiffness of the structure.

Figure 3b shows the plot of the anchoring elements circular frequencies, ordered in an ascendent way. The anchoring elements located in the "plateau region" of the seabed (see Figure 2) are characterized by the lowest circular frequencies, being their chord length the longest of the whole mooring system. These anchors might encounter high level of vibrations induced by the motion of the tunnel both for the case of simple resonance, occurring for "extreme" hydrodynamic events, and for the case of parametric resonance, which may arise if "ordinary" waves associated to the service life of the structure are considered. In fact, the frequencies corresponding to the highest spectral ordinates in the wave elevation spectrum (for H_s = 5 m) are close to two times the first natural frequency of these tethers. Proceeding towards the right direction of the abscissa axis, one may find two sets of circular frequencies, respectively denoted as SR1 and SR2. These sets of tethers might be susceptible of simple resonance phenomenon induced respectively by the hydrodynamic motion of the tunnel, whenever "extreme" waves and "ordinary" waves are considered. Finally, the last two circular frequencies correspond to the stiffest anchoring elements, having shortest chord length, which are located very close to the right and left shore, respectively. However, no significant dynamic amplification phenomena are expected in this case, since the natural circular frequencies of these tethers are sufficiently far from the first one of the tunnel. Additionally, it is worth noticing that the first mode of the tunnel is always expected to have a node very close to the position of these two tethers (see Figure 4b).

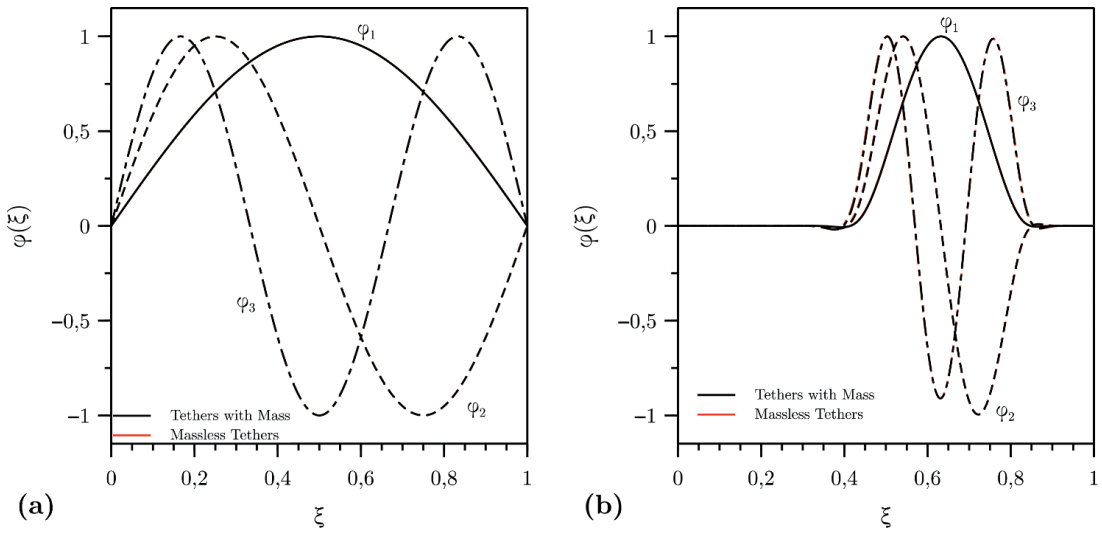

Figure 4. First three mode shapes of the tunnel for a constant (a) and variable (b) seabed depth profile. The non-dimensional abscissa of the tunnel is denoted as $\xi = x_T/L_T$.

Figure 4a and 4b shows the first three global modes of the SFT for a constant and variable seabed depth profile, respectively. As already evidenced in (Foti et al. 2023), the variable seabed profile (which consequently induces a spatially variable mooring stiffness profile) is responsible for the mode localization phenomena, around the region of highest flexibility of the mooring system. As long as the mooring stiffness is constant, localization phenomena do not occur and the mode shapes of the SFT preserve a global character (see Figure 4a). On the contrary, if the mooring stiffness is variable, the mode shapes localize in the range of lowest

stiffness, which is not located symmetrically with respect to the midspan but coincides with the "plateau" region (see Figure 4b – cf. Figure 2).

Moreover, it is noted that the influence of the anchoring elements' mass on the mode shapes is practically negligible for both seabed profiles. This evidence, together with results obtained in Figure 3, permits to conclude that it is feasible to assess the global dynamic response of the SFT by resorting to the simplified model of Euler-Bernoulli beam on a Winkler's bed (possessing a non-homogenous stiffness of the springs), and therefore, neglecting the mass of the tethers (see also (Foti et al. 2022) and Figure 1b).

5 CONCLUSIONS

In this paper, a dynamic substrucuring technique for Submerged Floating Tunnels (SFTs) was presented. The mooring system was modeled as a discrete series of anchoring elements individually described by a taut-string possessing axial extensibility, while the tunnel was modeled as a Euler-Bernoulli beam. The degrees of freedom at the interface between the tunnel and the anchors were evidenced, by expressing their value through the displacements of the tunnel. The inertially-coupled system was assembled and undamped free vibrations of the global structure were studied. The results showed the influence of both the variable mooring stiffness and the anchoring elements' mass on the global modes of the SFT. The classification of the motion regimes for the proposal of the Messina's strait SFT highlighted that the response of the tunnel to hydrodynamic loading conditions can be regarded as quasi-static. For this reason, it is feasible to address the global response of the system by relying on the simplified assumption of mass-less elastic tendon for the anchoring elements, which amounts to consider the tunnel as a Euler-Bernoulli beam resting on a non-homogenous Winkler-type soil. As per the anchoring elements, classification of the motion regimes has revealed the possibility of different resonance phenomena (both simple and parametric) under hydrodynamic loading conditions. Further research is currently ongoing to assess the role of geometrical nonlinearities of the anchoring elements on the global response on the SFT, and to include system coupling due to hydrodynamic loading of the tunnel itself, which may cause parametric excitation (and possibly, parametric resonance) of some tethers.

REFERENCES

Ahrens, D. 1997. Submerged floating tunnels - a concept whose time has arrived. *Tunneling and Underground Space Technology* 12: 318–336.

Bruschi, R. & Giardinieri, V. & Marazza, R. & Merletti, T. 1990. Submerged buoyant anchored tunnels: technical solutions for the fixed link across the strait of Messina, Italy. In J. Krokeborg (ed) *Strait crossings*: 605–612. Rotterdam: Balkema.

Chakrabarti, S.K. 1987. *Hydrodynamics of offshore structures*. Berlin: Computational Mechanics Publications, Springer.

Clough, R. & Penzien, J. 2003. *Dynamics of structures*, 3rd edn. Berkeley: Computers and Structures Inc.

Foti, F. & Martinelli L. & Perotti, F. 2022. A semi-analytical model for the design and optimization of SFTs under seismic loading. In J.R. Casas & D.M. Frangopol & J. Turmo (eds) *Bridge safety, maintenance, management, life-cycle, resilience and sustainability*: 1117–1121. CRC Press.

Foti, F. & Martinelli, L. & Morleo, E. & Perotti, F. 2023. Dynamic response of submerged floating tunnels: an enhanced semi-analytical approach. Submitted to *Ocean Engineering*, p 24.

Irvine, H.M. 1981. *Cable structures*. Cambridge, Massachusetts: The MIT Press series in structural mechanics.

Jakobsen, B. 2010. Design of the submerged floating tunnel operating under various conditions. *Procedia Engineering* 4: 71–79.

Perotti, F. & Foti, F. & Martinelli, L. & Tomasin, M. 2018. SFTs under dynamic loads: new design issues and numerical simulation. In N. Powers & D.M. Frangopol & R. Al-Mahaidi & C. Caprani (eds) *Maintenance, safety, risk, management and life-cycle performance of bridges*: 885–892. CRC Press.

Warnitchai, P. & Fujino, Y. & Susumpow, T. 1995. A non-linear dynamic model for cables and its application to a cable-structure system. *Journal of Sound and Vibration* 187(4): 695–712.

Wilson, J.F. 1984. *Dynamics of offshore structures*. Hoboken: Wiley Inc.